

# Ruthenium Silyl Complexes Containing the Cp(PMe<sub>3</sub>)<sub>2</sub>Ru Moiety: Preparation, Substituent Effects, and Silylene Character in the Ru–Si Bond

Frederick R. Lemke\*

Department of Chemistry and Biochemistry, Ohio University, Athens, Ohio 45701-2979

Kevin J. Galat and Wiley J. Youngs<sup>§</sup>

Department of Chemistry, The University of Akron, Akron, Ohio 44325-3601

Received November 25, 1998

The preparation and characterization of new ruthenium(II) silyl complexes containing the Cp(PMe<sub>3</sub>)<sub>2</sub>Ru moiety are described. The ruthenium(II) hydride Cp(PMe<sub>3</sub>)<sub>2</sub>RuH reacts with a variety of chlorosilanes to produce the ruthenium(II) silyl complexes Cp(PMe<sub>3</sub>)<sub>2</sub>RuSiR<sub>3</sub> [SiR<sub>3</sub> = SiCl<sub>3</sub> (**1**), SiHCl<sub>2</sub> (**2**), SiH<sub>2</sub>Cl (**3**), SiMeCl<sub>2</sub> (**4**), SiMeHCl (**5**), SiMe<sub>2</sub>Cl (**6**)] and the ruthenium(IV) dihydride [Cp(PMe<sub>3</sub>)<sub>2</sub>RuH<sub>2</sub>]Cl. Silyl complexes **1–6** undergo chloride/hydride exchange with LiAlH<sub>4</sub> to give the corresponding ruthenium(II) hydrosilyl complexes Cp(PMe<sub>3</sub>)<sub>2</sub>RuSiHR<sub>2</sub> [SiHR<sub>2</sub> = SiH<sub>3</sub> (**7**), SiMeH<sub>2</sub> (**8**), SiMe<sub>2</sub>H (**9**)]. Methylation of **6** with AlMe<sub>3</sub> produces Cp(PMe<sub>3</sub>)<sub>2</sub>RuSiMe<sub>3</sub> (**10**). A method for recovering the Cp(PMe<sub>3</sub>)<sub>2</sub>Ru moiety is described. The structure of **1** was determined by X-ray crystallography. Complexes **1–10** represent the first complete set of metal silicon compounds that contain every possible combination of H, Cl, and Me groups on silicon. The effects of the substituents on the spectroscopic properties of **1–10** were examined as a function of Tolman's electronic parameter ( $\chi_i$ ) for the substituents on silicon. The infrared stretching frequency,  $\nu(\text{Si-H})$ , and the NMR coupling constants,  $^2J_{\text{SiP}}$  and  $^1J_{\text{SiH}}$ , exhibit a linear relationship with  $\sum\chi_i$ , consistent with Bent's rule. However, when the NMR resonances SiR<sub>3</sub>  $\delta(^{29}\text{Si})$ , SiH  $\delta(^1\text{H})$ , and SiMe  $\delta(^{13}\text{C})$  were examined as a function of  $\sum\chi_i$ , the silyl groups differentiated into three classes: dichlorosilyl, monochlorosilyl, and "non-chlorosilyl"; within each class a linear but inverse relationship with  $\sum\chi_i$  was observed. Silylene character in the Ru–Si bond resulting from d(Ru)– $\sigma^*(\text{Si-Cl})$   $\pi$ -back-bonding interactions was used to explain the origin of the three silyl classes.

## Introduction

The chemistry of transition metal silicon compounds continues to generate considerable attention and interest.<sup>1–5</sup> The diverse developments in this field indicate the extensive interest in the catalytic and stoichiometric chemistry of metal–silicon-bonded compounds. Metal silicon compounds play prominent roles in a variety of metal-catalyzed organosilicon transformations such as hydrosilylation,<sup>6–8</sup> dehydrogenative silylation,<sup>9,10</sup> dehydrogenative coupling of hydrosilanes,<sup>11</sup> and silane re-

distributions.<sup>12</sup> Investigations into the chemistry of functionalized metal silicon complexes, L<sub>n</sub>M–SiR<sub>3–m</sub>X<sub>m</sub> ( $m = 1–3$ ; X = H, halogen, OTf, SAR; R = alkyl, aryl), have indicated a number of useful transformations involving the metal–silicon bond. Nucleophilic or radical-based substituent exchange reactions can generate new metal–silicon complexes.<sup>13</sup> Abstraction (and in some cases addition) of a group can generate complexes containing reactive silicon species (e.g., silylene, SiR<sub>2</sub>;  $\eta^2$ -silenes, R'<sub>2</sub>C=SiR<sub>2</sub>;  $\eta^2$ -hydrosilanes, H–SiR<sub>3</sub>)<sup>14–18</sup> as ligands; many of these species have been invoked as intermediates in catalytic and stoichiometric reactions of organosilanes.

<sup>§</sup> To whom correspondence should be addressed concerning X-ray structure determinations.

- (1) Tilley, T. D. In *The Silicon-Heteroatom Bond*; Patai, S., Rappoport, Z., Eds.; John Wiley & Sons: New York, 1991; pp 245–307.
- (2) Tilley, T. D. In *The Silicon-Heteroatom Bond*; Patai, S., Rappoport, Z., Eds.; John Wiley & Sons: New York, 1991; pp 309–364.
- (3) Sharma, H. K.; Pannell, K. H. *Chem. Rev.* **1995**, *95*, 1351–1374.
- (4) Schubert, U. *Adv. Organomet. Chem.* **1990**, *30*, 151–187.
- (5) Corey, J. Y.; Braddock-Wilking, J. *Chem. Rev.* **1999**, *99*, 175–292.
- (6) Ojima, I. In *The Chemistry of Organic Silicon Compounds*; Patai, S., Rappoport, Z., Eds.; John Wiley & Sons: New York, 1989; pp 1479–1526.
- (7) Harrod, J. F. In *Encyclopedia of Inorganic Chemistry*; King, R. B., Ed.; Wiley: Chichester, 1994; Vol. 3; pp 1486–1496.
- (8) Speier, J. L. *Adv. Organomet. Chem.* **1979**, *17*, 407–447.
- (9) Christ, M. L.; Sabo-Etienne, S.; Chaudret, B. *Organometallics* **1995**, *14*, 1082–1084.
- (10) Ezbiansky, K.; Djurovich, P. I.; LaForest, M.; Sinning, D. J.; Zayes, R.; Berry, D. H. *Organometallics* **1998**, *17*, 1455–1457.

- (11) Tilley, T. D. *Comments Inorg. Chem.* **1990**, *10*, 37–51.
- (12) Curtis, M. D.; Epstein, P. S. *Adv. Organomet. Chem.* **1981**, *19*, 213–255.
- (13) Malisch, W.; Thum, G.; Wilson, D.; Lorz, P.; Wachtler, U.; Seelbach, W. In *Silicon Chemistry*; Corey, J. Y., Corey, E. R., Gaspar, P. P., Eds.; Ellis Horwood Limited: Chichester, West Sussex, England, 1988; pp 327–335.
- (14) Zybilla, C.; Handwerker, H.; Friedrich, H. *Adv. Organomet. Chem.* **1994**, *36*, 229–281.
- (15) Zybilla, C. *Top. Curr. Chem.* **1992**, *160*, 1–45.
- (16) Tilley, T. D.; Campion, B. K.; Grumbine, S. D.; Straus, D. A.; Heyn, R. H. In *Frontiers of Organosilicon Chemistry*; Bassindale, A. R., Gaspar, P. P., Eds.; The Royal Society of Chemistry: Cambridge, 1991; pp 295–306.
- (17) Lickiss, P. D. *Chem. Soc. Rev.* **1992**, 271–279.
- (18) Lemke, F. R. *J. Am. Chem. Soc.* **1994**, *116*, 11183–11184.

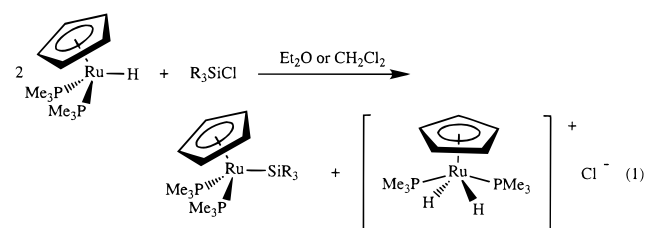
Functionalized transition metal silyl complexes have been conveniently prepared by the oxidative-addition of hydrosilanes to electron-rich metal centers which either possess a vacant coordination site or are accompanied by loss of a small molecule ( $H_2$ , alkane, etc.). The reaction of a variety of hydrosilanes ( $HSiX_3$ ) with the metal(II) alkyl complexes  $Cp'(PR_3)_2MR'$  ( $Cp' = Cp, Cp^*$ ;  $PR_3 = PMe_3, PPh_3$ ;  $M = Ru, Os$ ;  $R' = Me, CH_2SiMe_3$ ) at elevated temperatures produced the metal(II) silyl  $Cp'(PR_3)_2MSiX_3$  and/or metal(IV) bis(silyl)  $Cp'(PR_3)_2MH(SiX_3)_2$  complexes with loss of alkane ( $R'H$ ).<sup>19–24</sup> The product distribution of the metal–silicon complexes depended on reaction conditions and the strength of the metal–phosphorus bond. Alternatively, the alkali halide elimination method, in which a metal anion reacts with a halosilane or a metal halide reacts with a silyl anion, has also proved a convenient route to functionalized transition metal silyl complexes. Malisch and co-workers successfully prepared a wide variety of late transition metal silyl complexes of the type  $L_nMSiX_3$  ( $ML_n = CpCr(CO)_3, CpMo(CO)_3, Cp^*Mo(CO)_3, CpMo(CO)_2(PMe_3), Cp^*Mo(CO)_2(PMe_3), CpW(CO)_3, Cp^*W(CO)_3, CpW(CO)_2(PMe_3), Cp^*W(CO)_2(PMe_3), CpFe(CO)_2, Cp^*Fe(CO)_2, CpRu(CO)_2, Cp^*Ru(CO)_2$ ;  $SiX_3 = SiHCl_2, SiHMeCl, SiHMe_2, SiPhHCl, SiPh_2H$ , etc.) by reacting metal anions with the corresponding chlorosilane in hydrocarbon solvent.<sup>25–30</sup> Controlled exchange reactions at silicon afforded a variety of metallohydrosilanes,<sup>27–30</sup> -fluorosilanes,<sup>31</sup> -aminosilanes,<sup>32,33</sup> -silanols,<sup>28,34–37</sup> and -alkoxysilanes.<sup>13</sup>

Herein, we describe the formation of chlorosilyl ruthenium complexes  $Cp(PMe_3)_2RuSiR_2Cl$  employing a little-used HCl elimination reaction between an electron-rich ruthenium hydride  $Cp(PMe_3)_2RuH$  and the corresponding chlorosilanes; the formation of some of these chlorosilyl ruthenium complexes has been previously communicated.<sup>18</sup> Subsequent derivatization of these chlorosilyl ruthenium complexes produces the first

complete series of metal silyl complexes that contain all possible combinations of H, Cl, and Me groups on silicon:  $Cp(PMe_3)_2RuSiR_3$  ( $SiR_3 = SiCl_3, SiHCl_2, SiH_2Cl, SiMeCl_2, SiMeHCl, SiMe_2Cl, SiH_3, SiMeH_2, SiMe_2H, SiMe_3$ ). Trends in the spectroscopic parameters (IR and multinuclear NMR) of this unique set of ruthenium silyl complexes are reported and analyzed in terms of electronic and structural features of the complexes. The probability of silylene character in the Ru–Si bond due to  $d(Ru)-\sigma^*(Si-Cl)$   $\pi$ -back-bonding is also discussed.

## Results and Discussion

**A. Synthesis of Ruthenium Silyl Complexes.** The ruthenium silyl complexes used in this study were prepared by several different methods. One method involved the reaction of  $Cp(PMe_3)_2RuH$  with chlorosilanes ( $R_3SiCl$ ) to produce a nearly equimolar mixture of  $Cp(PMe_3)_2RuSiR_3$  and  $[Cp(PMe_3)_2RuH_2]Cl$  (eq 1).<sup>38,39</sup>



$SiR_3 = SiCl_3$  (1),  $SiHCl_2$  (2),  $SiH_2Cl$  (3),  $SiMeCl_2$  (4),  $SiMeHCl$  (5),  $SiMe_2Cl$  (6)

The chlorosilanes ( $SiCl_4, SiHCl_3$ , and  $SiH_2Cl_2$ ) were much more reactive toward  $Cp(PMe_3)_2RuH$  than the chloromethylsilanes ( $SiMeCl_3, SiMeHCl_2, SiMe_2Cl_2$ ). Addition of  $SiCl_4, SiHCl_3$ , or  $SiH_2Cl_2$  to a yellow solution of  $Cp(PMe_3)_2RuH$  in  $Et_2O$  at  $-78^\circ C$  resulted in the immediate formation of  $[Cp(PMe_3)_2RuH_2]Cl$  as a white precipitate and a light yellow solution of  $Cp(PMe_3)_2RuSiR_3$  [ $SiR_3 = SiCl_3$  (1),  $SiHCl_2$  (2),  $SiH_2Cl$  (3)]. Under similar conditions, the chloromethylsilanes showed little or no reaction with  $Cp(PMe_3)_2RuH$  in  $Et_2O$ , even after a day at room temperature. However, the chloromethylsilanes did readily react with  $Cp(PMe_3)_2RuH$  in  $CH_2Cl_2$  to give  $Cp(PMe_3)_2RuSiR_3$  [ $SiR_3 = SiMeCl_2$  (4),  $SiMeHCl$  (5),  $SiMe_2Cl$  (6)] and  $[Cp(PMe_3)_2RuH_2]Cl$  (eq 1). Regardless of the solvent used, the ruthenium silyl complexes 1–6 were obtained as light to dark yellow, air- and water-sensitive solids in good yields. The more substituted chloromethylsilanes  $SiMe_2HCl$  and  $SiMe_3Cl$  did not react with  $Cp(PMe_3)_2RuH$  even in  $CH_2Cl_2$ .

In the reaction of  $Cp(PMe_3)_2RuH$  with chlorosilanes, the white, air-sensitive dihydride complex  $[Cp(PMe_3)_2RuH_2]Cl$ <sup>38,39</sup> was sometimes obtained in yields of  $>100\%$ , based on the stoichiometry described in eq 1. These unusual yields of  $[Cp(PMe_3)_2RuH_2]Cl$  can be rationalized by the sensitivity of chlorosilanes to trace amounts of water. Hydrolysis of the chlorosilane would have produced HCl, which readily protonated  $Cp(PMe_3)_2RuH$  to give  $[Cp(PMe_3)_2RuH_2]Cl$ .<sup>38</sup> This hydrolysis problem was overcome by conducting the reaction of  $Cp(PMe_3)_2RuH$  with chlorosilanes in the presence of an added base such as  $NEt_3$  (eq 2). By this method, ruthenium

(19) Lemke, F. R.; Simons, R. S.; Youngs, W. J. *Organometallics* **1996**, *15*, 216–221.

(20) Lemke, F. R.; Chaitheerapapkul, C. *Polyhedron* **1996**, *15*, 2559–2565.

(21) Straus, D. A.; Tilley, T. D.; Rheingold, A. J.; Geib, S. J. *J. Am. Chem. Soc.* **1987**, *109*, 5872–5873.

(22) Straus, D. A.; Zhang, C.; Quimbita, G. E.; Grumbine, S. D.; Heyn, R. H.; Tilley, T. D.; Rheingold, A. L.; Geib, S. J. *J. Am. Chem. Soc.* **1990**, *112*, 2673–2681.

(23) Grumbine, S. K.; Straus, D. A.; Tilley, T. D. *Polyhedron* **1995**, *14*, 127–148.

(24) Wanandi, P. W.; Tilley, T. D. *Organometallics* **1997**, *16*, 4299–4313.

(25) Malisch, W.; Kuhn, M. *Chem. Ber.* **1974**, *107*, 979–995.

(26) Malisch, W.; Kuhn, M. *Chem. Ber.* **1974**, *107*, 2835–2851.

(27) Schmitzer, S.; Weis, U.; Kab, H.; Buchner, W.; Malisch, W.; Polzer, T.; Posset, U.; Keifer, W. *Inorg. Chem.* **1993**, *32*, 303–309.

(28) Malisch, W.; Lankat, R.; Fey, O.; Reising, J.; Schmitzer, S. *J. Chem. Soc., Chem. Commun.* **1995**, 1917–1919.

(29) Malisch, W.; Lankat, R.; Schmitzer, S.; Pikel, R.; Posset, U.; Kiefer, W. *Organometallics* **1995**, *14*, 5622–5627.

(30) Malisch, W.; Möller, S.; Fey, O.; Wekel, H.-U.; Pikel, R.; Posset, U.; Kiefer, W. *J. Organomet. Chem.* **1996**, *507*, 117–124.

(31) Malisch, W. *Chem. Ber.* **1974**, *107*, 3835–3849.

(32) Thum, G.; Ries, W.; Greissing, D.; Malisch, W. *J. Organomet. Chem.* **1983**, *252*, C67–C72.

(33) Thum, G.; Malisch, W. *J. Organomet. Chem.* **1984**, *264*, C5–C9.

(34) Adam, W.; Azzena, U.; Prechtel, F.; Hindahl, K.; Malisch, W. *Chem. Ber.* **1992**, *125*, 1409–1411.

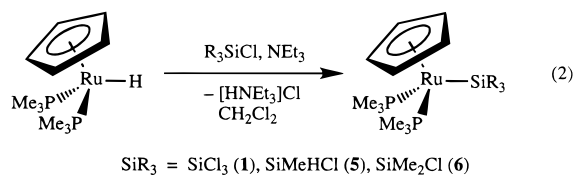
(35) Malisch, W.; Lankat, R.; Schmitzer, S.; Reising, J. *Inorg. Chem.* **1995**, *34*, 5701–5702.

(36) Malisch, W.; Schmitzer, S.; Lankat, R.; Neumayer, M.; Prechtel, F.; Adam, W. *Chem. Ber.* **1995**, *128*, 1251–1255.

(37) Möller, S.; Fey, O.; Malisch, W.; Seelbach, W. *J. Organomet. Chem.* **1996**, *507*, 239–244.

(38) Lemke, F. R.; Brammer, L. *Organometallics* **1995**, *14*, 3980–3987.

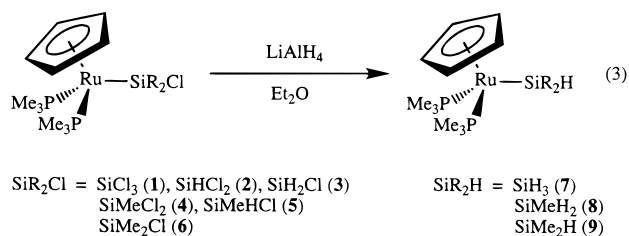
(39) Brammer, L.; Klooster, W. T.; Lemke, F. R. *Organometallics* **1996**, *15*, 1721–1727.



silyl complexes **1**, **5**, and **6** were obtained in high yields (>90%) with the added advantage that all of the ruthenium moiety ends up in the silyl complex (compared to eq 1).

The mechanism for the reaction of  $\text{Cp}(\text{PMe}_3)_2\text{RuH}$  with chlorosilanes has been discussed in detail<sup>18</sup> and will therefore only be briefly described here. The chlorosilanes undergo a nucleophilic attack by  $\text{Cp}(\text{PMe}_3)_2\text{RuH}$  with subsequent loss of HCl to give the ruthenium silyl complexes **1–6**. Concomitant protonation of a base, either  $\text{Cp}(\text{PMe}_3)_2\text{RuH}$  or  $\text{NEt}_3$ , removes the liberated HCl from the system. HCl elimination reactions to form metal silyl complexes have been used only to a limited extent, and most of these involved a metal chloride reacting with a hydrosilane. Chatt and co-workers reported the reaction of triarylsilanes,  $\text{Ar}_3\text{SiH}$  ( $\text{Ar} = \text{C}_6\text{H}_4\text{X}$ ,  $\text{X} = \text{H}, \text{F}, \text{Cl}, \text{CF}_3, \text{Me}, \text{OMe}, \text{NMe}_2$ ), with  $\text{PtX}_2(\text{EMe}_2\text{Ph})_2$  ( $\text{E} = \text{P}, \text{As}$ ) in the presence of  $\text{Et}_3\text{N}$  to form  $\text{PtX}(\text{SiAr}_3)(\text{EMe}_2\text{Ph})_2$  in 70–95% yields.<sup>40</sup>  $(\eta^7\text{-C}_7\text{H}_7)\text{Mo}(\text{CO})_2\text{SiCl}_3$  was prepared in 35% yield from  $(\eta^7\text{-C}_7\text{H}_7)\text{Mo}(\text{CO})_2\text{Cl}$  and  $\text{HSiCl}_3$  in the presence of  $\text{Et}_3\text{N}$ .<sup>41</sup> The reactions described in eqs 1 and 2 represent an example of a metal hydride reacting with chlorosilanes to form metal silyl complexes by HCl elimination. The only other reported HCl elimination reaction involving a metal hydride with a chlorosilane was the intramolecular formation of the metallocycle  $(\text{CO})_4\text{Mn}(\text{PMe}_2\text{-CH}_2\text{CH}_2\text{SiCl}_2)$  (30% yield) from  $(\text{CO})_4\text{MnH}(\text{PMe}_2\text{CH}_2\text{-CH}_2\text{SiCl}_3)$  in the presence of  $\text{Et}_3\text{N}$ .<sup>42</sup>

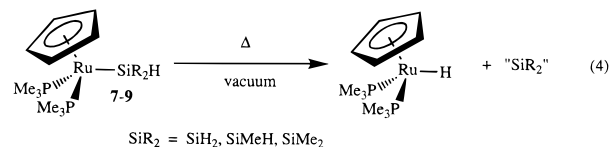
The ruthenium hydrosilyl complexes  $\text{Cp}(\text{PMe}_3)_2\text{RuSiR}_2\text{H}$  [ $\text{SiR}_2\text{H} = \text{SiH}_3$  (**7**),  $\text{SiMeH}_2$  (**8**),  $\text{SiMe}_2\text{H}$  (**9**)] were prepared by a chloride/hydride exchange of the corresponding chlorosilyl complexes **1–6** with  $\text{LiAlH}_4$  in  $\text{Et}_2\text{O}$  (eq 3). These hydrosilyl ruthenium complexes



**7–9** were isolated from solution in good yields (80–90%) as white or yellow, air-sensitive, waxy solids. No evidence for Ru–Si bond cleavage upon treatment of **1–9** with excess  $\text{LiAlH}_4$  was observed (i.e., formation of  $\text{Cp}(\text{PMe}_3)_2\text{RuH}$  and the corresponding hydrosilane).<sup>43</sup> Complexes **7–9** were soluble in common organic solvents but susceptible to hydride/chloride metathesis in chlorocar-

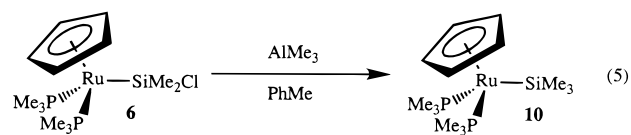
bon solvents ( $\text{CHCl}_3$  at 50 °C,  $\text{CH}_2\text{Cl}_2$  to a much lesser extent). Complexes **7–9** slowly decomposed in the solid state even when stored under an inert atmosphere.

Sublimation (80 °C, < 0.03 mmHg) can also be used to isolate complexes **7–9**, but this method of isolation is complicated by a fragmentation of the hydrosilyl group during the sublimation process. This fragmentation involves loss of silylene ( $\text{SiMe}_2$ ,  $\text{SiMeH}$ , or  $\text{SiH}_2$ ) with formation of the sublimable hydride  $\text{Cp}(\text{PMe}_3)_2\text{-RuH}$  (eq 4). The susceptibility of these hydrosilyl



ruthenium complexes to silylene loss during sublimation increases as the number of methyl groups on silicon increases:  $\text{SiH}_3 \leq \text{SiMeH}_2 < \text{SiMe}_2\text{H}$ .<sup>44</sup>

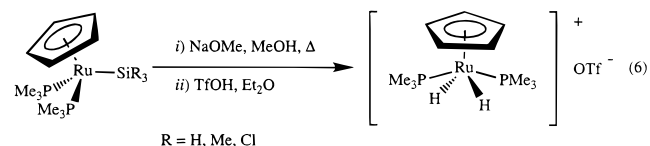
Since  $\text{SiMe}_3\text{Cl}$  does not react with  $\text{Cp}(\text{PMe}_3)_2\text{RuH}$ , an alternative route to  $\text{Cp}(\text{PMe}_3)_2\text{RuSiMe}_3$  (**10**) was used which involved the reaction of **6** with  $\text{AlMe}_3$  in toluene at room temperature (eq 5). Sublimation (80–100 °C,



<0.03 mmHg) of the reaction residue gave **10** (as a yellow-orange solid in good yields. Complex **10** can also be prepared by the reaction of **6** with  $\text{LiMe}$  in refluxing toluene; however, isolation of **10** from this reaction mixture was not as simple and clean as the reaction described in eq 5.

The ruthenium silyl complexes **1–10** prepared according to eqs 1–3 and 5 were characterized by multinuclear NMR and IR spectroscopies, mass spectrometry, and elemental analyses. The NMR and IR spectroscopic data are listed in Table 1, with the mass spectrometry and elemental analysis data listed in Table 2. The spectroscopic and analytical data are consistent with the  $\text{Cp}(\text{PMe}_3)_2\text{RuSiR}_3$  formulation of these complexes.

The  $\text{Cp}(\text{PMe}_3)_2\text{Ru}$  moiety was recovered through treatment of the ruthenium silyl complexes as described in eq 6. The first step involved the reaction of the



ruthenium silyl complexes with methoxide in refluxing methanol. In this step, the chlorosilyl ruthenium com-

(40) Chatt, J.; Eaborn, C.; Ibekwe, S. D.; Kapoor, P. N. *J. Chem. Soc. (A)* **1970**, 1343–1351.

(41) Isaacs, E. E.; Graham, W. A. G. *Can. J. Chem.* **1975**, *53*, 975–978.

(42) Grobe, J.; Walter, A. *J. Organomet. Chem.* **1977**, *140*, 325–348.

(43) The W–Si bond in  $\text{Cp}'(\text{CO})_3\text{WSiHCl}_2$  ( $\text{Cp}' = \text{Cp}, \text{Cp}^*$ ) was cleaved by  $\text{LiAlH}_4$  into  $\text{SiH}_4$  and  $\text{Li}[\text{Cp}'\text{W}(\text{CO})_3]$ . On the other hand, a  $\text{PMe}_3$  ligand in the tungsten coordination sphere stabilized the W–Si bond such that  $\text{Cp}^*(\text{CO})_2(\text{PMe}_3)\text{WSiR}_2\text{Cl}$  ( $\text{SiR}_2\text{Cl} = \text{SiHCl}_2, \text{SiMeHCl}$ ) gave the corresponding hydrosilyl complexes  $\text{Cp}^*(\text{CO})_2(\text{PMe}_3)\text{WSiR}_2\text{H}$  ( $\text{SiR}_2\text{H} = \text{SiH}_3, \text{SiMeH}_2$ ) upon treatment with  $\text{LiAlH}_4$ .<sup>27</sup>

(44) The susceptibility of the hydrosilanes  $\text{Cp}(\text{PMe}_3)_2\text{RuSiR}_2\text{H}$  ( $\text{SiR}_2\text{H} = \text{SiH}_3, \text{SiMeH}_2, \text{SiMe}_2\text{H}$ ) to silylene loss during sublimation parallels the preference for silylene loss observed in a mass spectral study of these hydrosilanes. Details of this mass spectral study will be reported in a later publication.



**Table 1. Multinuclear NMR and Infrared Spectroscopic Data and Electronic Factors for Ruthenium Silyl Complexes**

complex	<sup>1</sup> H NMR (ppm) <sup>a</sup>	<sup>13</sup> C{ <sup>1</sup> H} NMR (ppm) <sup>b</sup>	<sup>29</sup> Si DEPT NMR (ppm) <sup>c</sup>	<sup>31</sup> P{ <sup>1</sup> H} NMR (ppm) <sup>d</sup>	$\nu(\text{Si-H})$ (cm <sup>-1</sup> ) <sup>e</sup>	$\sum\chi_f$ <sup>f</sup>
Cp(PMe <sub>3</sub> ) <sub>2</sub> RuSiCl <sub>3</sub> ( <b>1</b> )	4.79 (s, 5H, Cp)	84.10 (t, $J_{\text{PC}} = 1.6$ Hz, Cp)	42.11 (t, $J_{\text{SiP}} = 43.6$ Hz)	9.33 (s, with <sup>29</sup> Si satellites $J_{\text{SiP}} = 43.7$ Hz)		44.4
	1.52 (fd, $N = 9.0$ Hz, 18H, PMe <sub>3</sub> )	24.69 (vt, $N = 32.0$ Hz, PMe <sub>3</sub> )				
Cp(PMe <sub>3</sub> ) <sub>2</sub> RuSiHCl <sub>2</sub> ( <b>2</b> )	6.41 (t, $J_{\text{PH}} = 3.3$ Hz, 1H, SiH)	83.66 (t, $J_{\text{PC}} = 1.6$ Hz, Cp)	66.79 (dt, $J_{\text{SiH}} = 199.6$ Hz, $J_{\text{SiP}} = 36.2$ Hz)	10.42 (s, with <sup>29</sup> Si satellites $J_{\text{SiP}} = 36.0$ Hz)	2073	37.9
	4.75 (s, 5H, Cp)	24.54 (vt, $N = 31.5$ Hz, PMe <sub>3</sub> )				
Cp(PMe <sub>3</sub> ) <sub>2</sub> RuSiH <sub>2</sub> Cl ( <b>3</b> )	1.46 (fd, $N = 8.9$ Hz, 18H, PMe <sub>3</sub> )	82.57 (t, $J_{\text{PC}} = 1.7$ Hz, Cp)	36.37 (tt, $J_{\text{SiH}} = 171.1$ Hz, $J_{\text{SiP}} = 32.9$ Hz)	11.50 (s, with <sup>29</sup> Si satellites $J_{\text{SiP}} = 33.2$ Hz)	2043	31.4
	5.34 (t, $J_{\text{PH}} = 3.7$ Hz, 2H, SiH)	24.62 (vt, $N = 31.0$ Hz, PMe <sub>3</sub> )				
Cp(PMe <sub>3</sub> ) <sub>2</sub> RuSiMeCl <sub>2</sub> ( <b>4</b> )	1.40 (fd, $N = 8.6$ Hz, 18H, PMe <sub>3</sub> )	83.03 (t, $J_{\text{PC}} = 1.6$ Hz, Cp)	92.16 (t, $J_{\text{SiP}} = 35.4$ Hz)	10.80 (s, with <sup>29</sup> Si satellites $J_{\text{SiP}} = 36.1$ Hz)		32.2
	4.72 (s, 5H, Cp)	25.15 (vt, $N = 31.1$ Hz, PMe <sub>3</sub> )				
Cp(PMe <sub>3</sub> ) <sub>2</sub> RuSiMeHCl ( <b>5</b> )	1.48 (fd, $N = 8.8$ Hz, 18H, PMe <sub>3</sub> )	82.38 (t, $J_{\text{PC}} = 1.7$ Hz, Cp)	57.17 (dt, $J_{\text{SiH}} = 163.6$ Hz, $J_{\text{SiP}} = 30.5$ Hz)	11.60 (AB, $J_{\text{PP}} = 38.9$ Hz, with <sup>29</sup> Si satellites $J_{\text{SiP}} = 31.1$ Hz)	2026	25.7
	0.97 (s, 3H, SiMe)	22.73 (s, SiMe)				
	5.45 (tq, $J_{\text{PH}} = 5.6$ Hz, $J_{\text{HH}} = 3.5$ Hz, 1H, SiH)	25.07 (dd, $J_{\text{PC}} = 27.4$ , 3.2 Hz, PMe <sub>3</sub> )				
	4.68 (s, 5H, Cp)	24.56 (dd, $J_{\text{PC}} = 27.5$ , 3.3 Hz, PMe <sub>3</sub> )				
	1.45 (d, $J_{\text{PH}} = 8.7$ Hz, 9H, PMe <sub>3</sub> )	12.16 (s, SiMe)				
Cp(PMe <sub>3</sub> ) <sub>2</sub> RuSiMe <sub>2</sub> Cl ( <b>6</b> )	1.37 (d, $J_{\text{PH}} = 8.3$ Hz, 9H, PMe <sub>3</sub> )	82.28 (t, $J_{\text{PC}} = 1.8$ Hz, Cp)	87.29 (t, $J_{\text{SiP}} = 30.2$ Hz)	11.83 (s, with <sup>29</sup> Si satellites $J_{\text{SiP}} = 30.5$ Hz)		20.0
	0.73 (d, $J_{\text{HH}} = 3.5$ Hz, 3H, SiMe)	25.81 (vt, $N = 29.9$ Hz, PMe <sub>3</sub> )				
Cp(PMe <sub>3</sub> ) <sub>2</sub> RuSiH <sub>3</sub> ( <b>7</b> )	0.58 (s, 6H, SiMe)	16.66 (s, SiMe)	-56.68 (qt, $J_{\text{SiH}} = 149.5$ Hz, $J_{\text{SiP}} = 32.4$ Hz)	12.02 (s, with <sup>29</sup> Si satellites $J_{\text{SiP}} = 31.9$ Hz)	2019	24.9
	4.59 (s, 5H, Cp)	81.08 (t, $J_{\text{PC}} = 1.9$ Hz, Cp)				
Cp(PMe <sub>3</sub> ) <sub>2</sub> RuSiMeH <sub>2</sub> ( <b>8</b> )	3.09 (t, $J_{\text{PH}} = 5.4$ Hz, 3H, SiH)	24.68 (vt, $N = 30.1$ Hz, PMe <sub>3</sub> )	-13.75 (tt, $J_{\text{SiH}} = 146.6$ Hz, $J_{\text{SiP}} = 29.9$ Hz)	12.41 (s, with <sup>29</sup> Si satellites $J_{\text{SiP}} = 30.0$ Hz)	1997	19.2
	1.36 (fd, $N = 8.6$ Hz, 18H, PMe <sub>3</sub> )	81.11 (t, $J_{\text{PC}} = 1.9$ Hz, Cp)				
Cp(PMe <sub>3</sub> ) <sub>2</sub> RuSiMe <sub>2</sub> H ( <b>9</b> )	4.58 (s, 5H, Cp)	24.79 (vt, $N = 29.6$ Hz, PMe <sub>3</sub> )	13.85 (dt, $J_{\text{SiH}} = 144.1$ Hz, $J_{\text{SiP}} = 26.9$ Hz)	12.29 (s, with <sup>29</sup> Si satellites $J_{\text{SiP}} = 26.7$ Hz)	1978	13.5
	0.26 (t, $J_{\text{HH}} = 4.3$ Hz, 3H, SiMe)	0.14 (t, $J_{\text{PC}} = 1.9$ Hz, SiMe)				
	4.56 (s, 5H, Cp)	81.04 (t, $J_{\text{PC}} = 1.9$ Hz, Cp)				
	3.94 (nonet, $J_{\text{HH}} \sim J_{\text{PH}} = 3.6$ Hz, 1H, SiH)	25.24 (vt, $N = 29.0$ Hz, PMe <sub>3</sub> )				
	1.36 (fd, $N = 8.4$ Hz, 18H, PMe <sub>3</sub> )	6.31 (t, $J_{\text{PC}} = 1.9$ Hz, SiMe)				
Cp(PMe <sub>3</sub> ) <sub>2</sub> RuSiMe <sub>3</sub> ( <b>10</b> )	0.24 (d, $J_{\text{HH}} = 3.8$ Hz, 6H, SiMe)		19.56 (t, $J_{\text{SiP}} = 26.0$ Hz)	12.61 (s, with <sup>29</sup> Si satellites $J_{\text{SiP}} = 25.8$ Hz)		7.8
	4.57 (s, 5H, Cp)	81.61 (t, $J_{\text{PC}} = 2.0$ Hz, Cp)				
	1.36 (fd, $N = 8.2$ Hz, 18H, PMe <sub>3</sub> )	26.48 (vt, $N = 27.7$ Hz, PMe <sub>3</sub> )				
	0.10 (s, 9H, SiMe)	11.22 (t, $J_{\text{PC}} = 1.4$ Hz, SiMe)				

<sup>a</sup> At 250 MHz and ambient probe temperature in CD<sub>2</sub>Cl<sub>2</sub> and referenced to residual proton peak (5.32 ppm). The PMe<sub>3</sub> resonances in these complexes appear as a A<sub>9</sub>XX'A<sub>9</sub> pattern in the form of a "filled-in-doublet" (fd) with the separation of the outer lines  $N = {}^2J_{\text{PH}} + {}^4J_{\text{PH}}$ . <sup>b</sup> At 62.9 MHz and ambient probe temperature in CD<sub>2</sub>Cl<sub>2</sub> and referenced to solvent (53.8 ppm). The PMe<sub>3</sub> resonances in these complexes appear as a "virtual triplet" (vt) with the separation of the outer lines  $N = {}^1J_{\text{PC}} + {}^3J_{\text{PC}}$ . <sup>c</sup> At 79.5 MHz and ambient probe temperature in CD<sub>2</sub>Cl<sub>2</sub> and referenced to external SiMe<sub>4</sub> (0.00 ppm). <sup>d</sup> At 101 MHz and ambient probe temperature in CD<sub>2</sub>Cl<sub>2</sub> and referenced to external H<sub>3</sub>PO<sub>4</sub> (85%, 0.00 ppm). <sup>e</sup> In CH<sub>2</sub>Cl<sub>2</sub>. <sup>f</sup> Summation of the Tolman's electronic parameters for the three substituents on silicon:  $\chi_f(\text{Cl}) = 14.8$ ,  $\chi_f(\text{H}) = 8.3$ ,  $\chi_f(\text{Me}) = 2.6$ .<sup>56</sup>

**Table 2. Analytical Data for Cp(PMe<sub>3</sub>)<sub>2</sub>RuSiR<sub>3</sub> Complexes**

SiR <sub>3</sub>	MS <sup>a</sup>	formula	C found (calcd), %	H found (calcd), %
SiCl <sub>3</sub> ( <b>1</b> )	454	C <sub>11</sub> H <sub>23</sub> Cl <sub>3</sub> P <sub>2</sub> RuSi	29.02 (29.18)	5.12 (5.12)
SiHCl <sub>2</sub> ( <b>2</b> )	418	C <sub>11</sub> H <sub>24</sub> Cl <sub>2</sub> P <sub>2</sub> RuSi	31.49 (31.58)	5.71 (5.78)
SiH <sub>2</sub> Cl ( <b>3</b> )	384	C <sub>11</sub> H <sub>25</sub> ClP <sub>2</sub> RuSi	34.28 (34.42)	6.54 (6.56)
SiMeCl <sub>2</sub> ( <b>4</b> )	432	C <sub>12</sub> H <sub>26</sub> Cl <sub>2</sub> P <sub>2</sub> RuSi	33.32 (33.34)	5.65 (6.06)
SiMeHCl ( <b>5</b> )	398	C <sub>12</sub> H <sub>27</sub> ClP <sub>2</sub> RuSi	35.53 (36.22)	6.57 (6.84)
SiMe <sub>2</sub> Cl ( <b>6</b> )	412	C <sub>13</sub> H <sub>29</sub> ClP <sub>2</sub> RuSi	37.75 (37.91)	7.10 (7.10)
SiH <sub>3</sub> ( <b>7</b> )	350	C <sub>11</sub> H <sub>26</sub> P <sub>2</sub> RuSi	37.67 (37.81)	7.32 (7.50)
SiMeH <sub>2</sub> ( <b>8</b> )	364	C <sub>12</sub> H <sub>28</sub> P <sub>2</sub> RuSi	39.24 (39.66)	7.84 (7.76)
SiMe <sub>2</sub> H ( <b>9</b> )	378	C <sub>13</sub> H <sub>30</sub> P <sub>2</sub> RuSi	41.98 (41.36)	8.21 (8.01)
SiMe <sub>3</sub> ( <b>10</b> )	392	C <sub>14</sub> H <sub>32</sub> P <sub>2</sub> RuSi	42.55 (42.95)	8.10 (8.24)

<sup>a</sup> Parent ion *m/z* in each case.

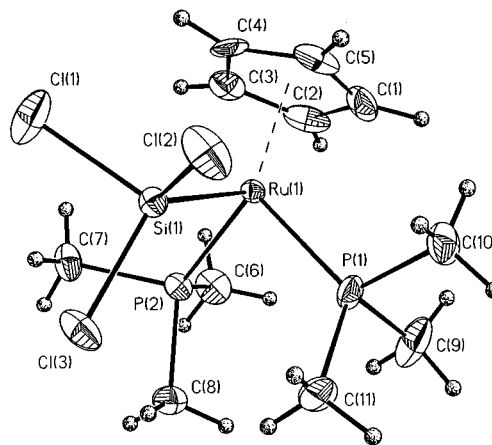
**Table 3. Selected Interatomic Distances (Å) and Angles (deg) for Cp(PMe<sub>3</sub>)<sub>2</sub>RuSiCl<sub>3</sub> (**1**)**

Interatomic Distances <sup>a</sup>			
Ru(1)–Si(1)	2.265(2)	Si(1)–Cl(1)	2.122(3)
Ru(1)–P(1)	2.273(2)	Si(1)–Cl(2)	2.114(3)
Ru(1)–P(2)	2.280(2)	Si(1)–Cl(3)	2.121(3)
Ru(1)–Cnt	1.887		
Bond Angles <sup>a</sup>			
P(1)–Ru(1)–P(2)	95.80(7)	P(1)–Ru(1)–Si(1)	92.60(7)
P–Ru(1)–Cnt	123.2 (av)	P(2)–Ru(1)–Si(1)	93.00(7)
Cnt–Ru(1)–Si(1)	121.2	Ru(1)–Si(1)–Cl(1)	116.8(1)
Ru(1)–Si(1)–Cl(2)	115.0(1)	Ru(1)–Si(1)–Cl(3)	125.6(1)
Cl(1)–Si(1)–Cl(2)	99.0(1)	Cl(1)–Si(1)–Cl(3)	96.9(1)
Cl(2)–Si(1)–Cl(3)	98.8(1)		

<sup>a</sup> Cnt = the centroid of the cyclopentadienyl ring.

plexes **1–6** were converted to the corresponding methoxysilyl complexes, while the nonchlorosilyl ruthenium complexes **7–10** were generally unaffected. Some Cp(PMe<sub>3</sub>)<sub>2</sub>RuH was also formed in this step, presumably due to Ru–Si bond cleavage. The Cp(PMe<sub>3</sub>)<sub>2</sub>Ru-containing products were isolated by sublimation. The second step involved treatment of the sublimate with triflic acid (TfOH) in Et<sub>2</sub>O. The triflic acid cleaved the Ru–Si bond to form Cp(PMe<sub>3</sub>)<sub>2</sub>RuH, which was readily protonated to afford the dihydride [Cp(PMe<sub>3</sub>)<sub>2</sub>RuH<sub>2</sub>]OTf with additional triflic acid. Conversion of the cationic dihydride [Cp(PMe<sub>3</sub>)<sub>2</sub>RuH<sub>2</sub>]<sup>+</sup> to the neutral monohydride Cp(PMe<sub>3</sub>)<sub>2</sub>RuH was readily accomplished with NaOMe in refluxing MeOH.<sup>38</sup> This provided a convenient method for the recovery of the Cp(PMe<sub>3</sub>)<sub>2</sub>Ru moiety as the neutral monohydride Cp(PMe<sub>3</sub>)<sub>2</sub>RuH.

**B. Structure of Cp(PMe<sub>3</sub>)<sub>2</sub>RuSiCl<sub>3</sub> (**1**).** The crystal structure of Cp(PMe<sub>3</sub>)<sub>2</sub>RuSiCl<sub>3</sub> (**1**) has been determined by X-ray diffraction at 141 K. Pertinent interatomic distances and angles for **1** are presented in Table 3. The molecular structure of **1** (Figure 1) confirms the formulation and connectivity of the ruthenium silyl complexes described in section A. Complex **1** adopts a “three-legged piano stool” geometry around ruthenium, with “legs” composed of one SiCl<sub>3</sub> and two PMe<sub>3</sub> groups. The bond distances and angles in the Cp(PMe<sub>3</sub>)<sub>2</sub> moiety are normal when compared to the structures of related Cp(PMe<sub>3</sub>)<sub>2</sub>RuX complexes.<sup>19,38,45–47</sup> The Ru–Si bond distance of 2.265(2) Å is consistent with a single bond. This Ru–Si bond distance lies on the low end of the range

**Figure 1.** Perspective view of the molecular structure of Cp(PMe<sub>3</sub>)<sub>2</sub>RuSiCl<sub>3</sub> (**1**). The thermal ellipsoids are drawn at the 50% probability level.

(2.27–2.51 Å) observed for other d<sup>6</sup> ruthenium silyl complexes<sup>1,2,19,22,23,48</sup> but is in the middle of the range (2.20–2.34 Å) observed for other group 8 trichlorosilyl complexes, L<sub>n</sub>MSiCl<sub>3</sub> (M = Fe,<sup>49–54</sup> Ru,<sup>48</sup> Os<sup>55</sup>). The Si–Cl bond distances in **1** [range 2.114–2.122 Å, 2.119 Å (av)] are significantly longer than the Si–Cl bond distances observed in the other group 8 trichlorosilyl complexes (range 2.026–2.090 Å). The short Ru–Si and long Si–Cl distances indicate a π-interaction between the ruthenium and the trichlorosilyl group (vide infra).

Complex **1** has a staggered conformation about the Ru–Si bond with the Cp and Cl(3) groups in an anti relationship (Cp centroid–Ru–Si–Cl(3) dihedral angle = 169.8°). The silyl group has a distorted tetrahedral geometry with an average Cl–Si–Cl angle of 98.2 ± 1.2°. By comparison, the average Ru–Si–Cl angle of 119.1 ± 5.7° is significantly larger but within the M–Si–Cl angle range (110–120°) observed for other group 8 trichlorosilyl complexes.<sup>48,49,53,55</sup> The Ru–Si–Cl(3) angle of 125.6(1)°, which is anti to the Cp group, lies noticeable outside the group 8 M–Si–Cl angle range. In other ruthenium silyl complexes, the Ru–Si–X angle for substituents anti to a Cp group have also been observed to be 10° or more larger than Ru–Si–X angles for the other substituents on silicon: Cp(PMe<sub>3</sub>)<sub>2</sub>RuSiCl<sub>2</sub>Cp\* [Ru–Si–Cl(anti) 119.9° vs Ru–Si–Cl 109.2°],<sup>19</sup> Cp\*(PMe<sub>3</sub>)<sub>2</sub>RuSiPh<sub>2</sub>H [Ru–Si–H(anti) 112.9° vs Ru–Si–Ph 98.8° (av)],<sup>22</sup> and Cp\*(PMe<sub>3</sub>)<sub>2</sub>RuSiPh<sub>2</sub>OTf [Ru–Si–OTf(anti) 118.2° vs Ru–Si–Ph 96.9° (av)].<sup>23</sup>

**C. Spectroscopic Trends.** The ruthenium silyl complexes **1–10** represent the first complete set of transition metal silicon complexes in which the substituents on silicon contain all possible combination of Cl,

(48) Einstein, F. W. B.; Jones, T. *Inorg. Chem.* **1982**, *21*, 987–990.

(49) Schubert, U.; Kraft, G.; Walther, E. *Z. Anorg. Allg. Chem.* **1984**, *519*, 96–106.

(50) Asirvatham, V. S.; Yao, Z.; Klabunde, K. J. *J. Am. Chem. Soc.* **1994**, *116*, 5493–5494.

(51) Yao, Z.; Klabunde, K. J.; Asirvatham, A. S. *Inorg. Chem.* **1995**, *34*, 5289–5294.

(52) Connolly, J. W.; Cowley, A. H.; Nunn, C. M. *Polyhedron* **1990**, *9*, 1337–1340.

(53) Manojlovic-Muir, L.; Muir, K. W.; Ibers, J. A. *Inorg. Chem.* **1970**, *9*, 447–452.

(54) Vancea, L.; Benneett, M. J.; Jones, C. E.; Smith, R. A.; Graham, W. A. G. *Inorg. Chem.* **1977**, *16*, 897–902.

(55) Hübler, K.; Hunt, P. A.; Maddock, S. M.; Rickard, C. E. F.; Roper, W. R.; Salter, D. M.; Schwerdtfeger, P.; Wright, L. J. *Organometallics* **1997**, *16*, 5076–5083.

(45) Lemke, F. R.; Szalda, D. J.; Bullock, R. M. *Organometallics* **1992**, *11*, 876–884.

(46) Lemke, F. R.; Szalda, D. J.; Bullock, R. M. *J. Am. Chem. Soc.* **1991**, *113*, 8466–8477.

(47) Bullock, R. M.; Lemke, F. R.; Szalda, D. J. *J. Am. Chem. Soc.* **1990**, *112*, 3244–3245.

H, and Me groups. This series of 10 ruthenium silyl complexes offers a unique opportunity to evaluate how changing the substituents on silicon influences the spectroscopic properties of these complexes. Since the  $\text{Cp}(\text{PMe}_3)_2\text{Ru}$  moiety is the same throughout this series, trends in the spectroscopic properties of complexes **1–10** should only arise from the steric and electronic effects of the Cl, H, and Me substituents on silicon. The cone angles for the silyl groups used in this study are relatively small, ranging from  $122^\circ$  for  $\text{SiCl}_3$  to  $118^\circ$  for  $\text{SiMe}_3$  to  $87^\circ$  for  $\text{SiH}_3$  (based on the assumption that the cone angles for the  $\text{SiX}_3$  groups are similar to the cone angles of the corresponding phosphines,  $\text{PX}_3$ ).<sup>56,57</sup> Therefore, the sterics of the silyl groups should not have a significant influence on the observed spectroscopic properties of the ruthenium silyl complexes and will not be considered any further. Only the effect of the electronic nature (electron-withdrawing ability) of the Cl, H, and Me groups on the spectroscopic properties of the ruthenium silyl complexes will be examined. Tolman's electronic parameter,  $\chi_i$ , will be used as a gauge of the electron-withdrawing ability of the substituents on silicon [ $\chi_i(\text{Me}) = 2.6$ ,  $\chi_i(\text{H}) = 8.3$ ,  $\chi_i(\text{Cl}) = 14.8$ ].<sup>56</sup> The summation of Tolman's electronic parameters for the three substituents on silicon,  $\sum\chi_i$ , represents the combined electron-withdrawing ability of the substituents on silicon.<sup>58</sup> The larger the  $\sum\chi_i$  value, the more electron-withdrawing the substituents on silicon. The  $\sum\chi_i$  values for the various silyl groups used in this study are listed in Table 1.

**1. Infrared Spectra.** The Si–H stretching frequencies for the ruthenium hydrosilyl complexes,  $\text{Cp}(\text{PMe}_3)_2\text{RuSiHR}_2$ , were observed in the 1975–2075  $\text{cm}^{-1}$  region. In comparison with nonmetalated silanes, the  $\nu(\text{Si–H})$  for these ruthenium hydrosilyl complexes are shifted to lower wavenumbers by 140–190  $\text{cm}^{-1}$  compared to the corresponding methylhydro- ( $\text{MeSiHR}_2$ ), dihydro- ( $\text{H}_2\text{SiR}_2$ ), and chlorohydrosilanes ( $\text{ClSiHR}_2$ ).<sup>59</sup> These relatively low  $\nu(\text{Si–H})$  values suggest significant hydride character for the SiH hydrogen, which is consistent with the hydride/chloride metathesis reactions in chlorocarbon solvents described in part A.<sup>26,27,31</sup>

A plot of  $\nu(\text{Si–H})$  as a function of  $\sum\chi_i$  for the ruthenium hydrosilyl complexes can be found in Figure 2. A linear relationship between  $\nu(\text{Si–H})$  and  $\sum\chi_i$  is observed and is consistent with Bent's rule.<sup>60</sup> According to Bent's rule and in the context of this study, a more electron-withdrawing substituent (i.e., Cl) requires more p character at the silicon atom for bonding, leaving more s character for the other atoms or groups bound to silicon (i.e., H, Me, and Ru). Thus, the Si–H bond strength and  $\nu(\text{Si–H})$  should increase with increasing

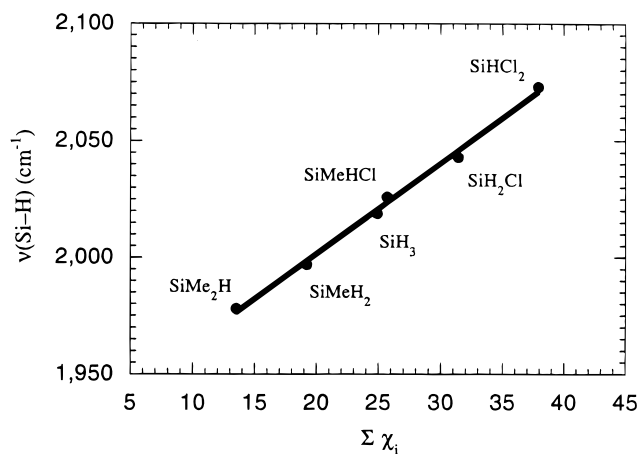


**Figure 2.**  $\nu(\text{Si–H})$  versus  $\sum\chi_i$  for the ruthenium hydrosilyl complexes  $\text{Cp}(\text{PMe}_3)_2\text{RuSiHR}_2$ : slope = 3.88  $\text{cm}^{-1}$  per  $\chi_i$  unit,  $R = 0.998$ .

$\sum\chi_i$  values. Complex **1**, which has the largest  $\sum\chi_i$  value also has the strongest Si–H bond (largest  $\nu(\text{Si–H})$  value at 2073  $\text{cm}^{-1}$ ), while complex **9**, with the smallest  $\sum\chi_i$  value, has the weakest Si–H bond ( $\nu(\text{Si–H}) = 1978$   $\text{cm}^{-1}$ ).

A similar linear relationship between  $\nu(\text{Si–H})$  and the electron-withdrawing ability of the other substituents on silicon has been observed for a variety of nonmetalated hydrosilanes,  $\text{HSiR}_3$  ( $R = \text{H, alkyl, Cl, F, Ph, OMe, NMe}_2$ ).<sup>59</sup> A general increase in  $\nu(\text{Si–H})$  was also observed in some iron, molybdenum, and tungsten hydrosilyl systems when a H or Me group was replaced with a Cl.<sup>25,27</sup> More detailed analyses of  $\nu(\text{Si–H})$  were hampered by a lack of metalated hydrosilyl complexes. The entirety of the ruthenium hydrosilyl series (**2, 3, 5, and 7–9**) allows, for the first time, a thorough examination of how  $\nu(\text{Si–H})$  is effected by the other substituents on silicon in metalated hydrosilanes.

**2. NMR Chemical Shifts.** The substituent effects on the chemical shifts of the NMR active nuclei in complexes **1–10** can be grouped into three classes: silicon, nuclei attached to silicon, and nuclei two or more bonds from silicon. The resonances for the silyl group in the  $^{29}\text{Si}$  NMR spectra of complexes **1–10** were observed over a 160 ppm range (Table 1). A plot of  $\delta(^{29}\text{Si})$  as a function of  $\sum\chi_i$  for complexes **1–10** is shown in Figure 3. The most striking feature of this plot is that the ruthenium silyl complexes are arranged into three silyl classes: a dichlorosilyl,  $\text{SiRCl}_2$  ( $R = \text{Cl, H, Me}$ ), class; a monochlorosilyl,  $\text{SiR}_2\text{Cl}$  ( $R = \text{H and/or Me}$ ), class; and a “non-chlorosilyl”,  $\text{SiR}_3$  ( $R = \text{H and/or Me}$ ), class. A couple of trends are observed from the plot in Figure 3. First, the silyl complexes within a class exhibit a linear relationship with respect to  $\sum\chi_i$ . Second, the silyl classes are nearly parallel with respect to each other. Third, within a silyl class,  $\delta(^{29}\text{Si})$  moves upfield with increasing  $\sum\chi_i$  (i.e., replacing a Me group with a H). Fourth, a general downfield shift in  $\delta(^{29}\text{Si})$  is observed upon going from one silyl class to another (i.e., replacement of a Me group or a H with Cl). Table 4 lists the effect of substituent changes on  $\delta(^{29}\text{Si})$ . Large standard deviation values ( $\pm 27$  ppm) are observed for the average  $\Delta\delta(^{29}\text{Si})$  of the H/Cl and Me/Cl exchanges. This is due to the fact that the magnitude of  $\Delta\delta(^{29}\text{Si})$  for the conversion between “non-chlorosilyl” and monochlorosilyl classes [ $\Delta\delta(^{29}\text{Si})$ ]

(56) Tolman, C. A. *Chem. Rev.* **1977**, *77*, 313–348.

(57) Tolman's  $\text{PX}_3$  cone angles may actually overestimate the  $\text{SiX}_3$  cone angles. On the basis of the method described by Tolman,<sup>56</sup> the  $\text{SiCl}_3$  cone angle in **1** was calculated to be  $115^\circ$  (compared to  $122^\circ$  for  $\text{PCl}_3$ ) using an average Ru–Si–Cl angle ( $119^\circ$ ), an average Si–Cl distance (2.12 Å), and the van der Waals radii of Cl (1.80 Å).

(58) Hammett  $\sigma_p$  or modified Taft  $\sigma^*(\text{Si})$ <sup>59</sup> parameters can also be used as a gauge of the electron-withdrawing ability of the substituents on silicon. Plots of the various spectroscopic properties as a function of  $\sum\sigma_p$  or  $\sum\sigma^*(\text{Si})$  for the substituents on silicon are very similar to the plots of these spectroscopic properties as a function of  $\sum\chi_i$ . The observed trends and relationships based on Hammett  $\sigma_p$  or modified Taft  $\sigma^*(\text{Si})$  parameters are the same as those observed using Tolman  $\chi_i$  parameters.

(59) Attridge, C. J. *J. Organomet. Chem.* **1968**, *13*, 259–262.

(60) Bent, H. A. *Chem. Rev.* **1961**, *61*, 276–311.



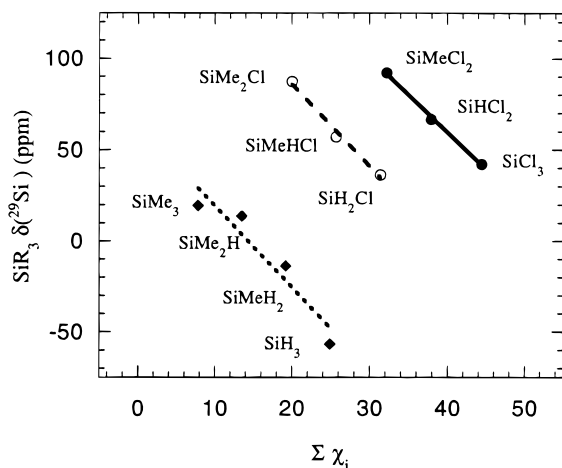


**Figure 3.**  $^{29}\text{Si}$  NMR chemical shift of the silyl group versus  $\Sigma\chi_i$  for the ruthenium silyl complexes  $\text{Cp}(\text{PMe}_3)_2\text{RuSiR}_3$  (**1–10**) showing the three silyl classes: dichlorosilyl (●, slope =  $-4.10$  ppm per  $\chi_i$  unit,  $R = 0.999$ ), monochlorosilyl (○, slope =  $-4.47$  ppm per  $\chi_i$  unit,  $R = 0.994$ ), and “non-chlorosilyl” (◆, slope =  $-4.50$  ppm per  $\chi_i$  unit,  $R = 0.950$ ).

**Table 4. Substituent Effects on the NMR Chemical Shifts and Coupling Constants of  $\text{Cp}(\text{PMe}_3)_2\text{RuSiR}_3$  Complexes 1–10**

R group	replace with	$\text{SiR}_3 \Delta\delta(^{29}\text{Si})$ (av, ppm) <sup>a</sup>	$\text{SiH} \Delta\delta(^1\text{H})$ (av, ppm) <sup>a</sup>	$\text{SiMe} \Delta\delta(^{13}\text{C})$ (av, ppm) <sup>a</sup>	$\Delta^1 J_{\text{SiH}}$ (av, Hz) <sup>b</sup>
Me	H	$-25.4 \pm 12.2$	$-0.32 \pm 0.27$	$-5.19 \pm 0.87$	$4.3 \pm 2.8$
H	Cl	$60.6 \pm 26.9^c$	$1.68 \pm 0.59$	$10.98 \pm 0.91$	$22.4 \pm 5.8$
Me	Cl	$35.1 \pm 27.0^d$	$1.36 \pm 0.35$	$5.79 \pm 0.32$	$26.7 \pm 8.5$

<sup>a</sup>  $\Delta\delta = \delta$  final complex  $- \delta$  initial complex. <sup>b</sup>  $\Delta^1 J_{\text{SiH}} = ^1 J_{\text{SiH}}$  final complex  $- ^1 J_{\text{SiH}}$  initial complex. <sup>c</sup> The  $\text{SiHCl}_2/\text{SiCl}_3$  conversion ( $\Delta\delta = -24.7$  ppm) was excluded from the average calculation. <sup>d</sup> The  $\text{SiMeCl}_2/\text{SiCl}_3$  conversion ( $\Delta\delta = -50.1$  ppm) was excluded from the average calculation.

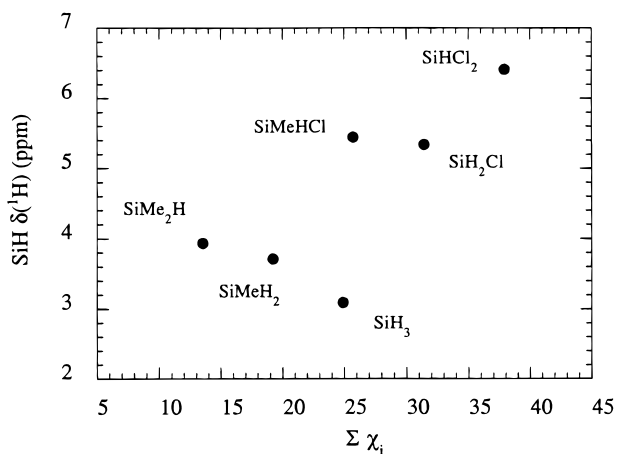


**Figure 4.**  $^1\text{H}$  NMR chemical shift of the SiH group versus  $\Sigma\chi_i$  for the ruthenium hydrosilyl complexes  $\text{Cp}(\text{PMe}_3)_2\text{-RuSiHR}_2$ .

$= 79.1 \pm 12.1$  ppm for H/Cl and  $53.7 \pm 12.6$  ppm for Me/Cl exchanges] is much larger than the magnitude of  $\Delta\delta(^{29}\text{Si})$  for the conversion between monochlorosilyl and dichlorosilyl classes [ $\Delta\delta(^{29}\text{Si}) = 32.7 \pm 3.2$  ppm for H/Cl and  $7.3 \pm 3.4$  ppm for Me/Cl exchanges].

The resonances for nuclei attached to silicon are also influenced by the other substituents on silicon. Figure 4 shows a plot of the  $\text{SiH} \delta(^1\text{H})$  as a function of  $\Sigma\chi_i$  for the ruthenium silyl complexes. In this plot, the ruthenium hydrosilyl complexes are arranged in a triangular

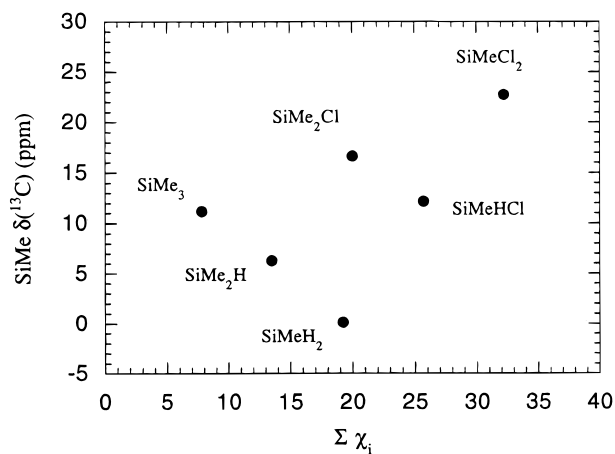


**Figure 5.**  $^{13}\text{C}$  NMR chemical shift of the SiMe group versus  $\Sigma\chi_i$  for the ruthenium methylsilyl complexes  $\text{Cp}(\text{PMe}_3)_2\text{RuSiMeR}_2$ .

formation which, as observed in Figure 3, can be grouped into the three silyl classes: dichlorosilyl, monochlorosilyl, and “non-chlorosilyl”.<sup>61</sup> Similarly, a plot of the  $\text{SiMe} \delta(^{13}\text{C})$  as a function of  $\Sigma\chi_i$  for the ruthenium methylsilyl complexes, Figure 5, exhibits the same three classes of silyl complexes in a triangular formation. Changes in the  $\text{SiH} \delta(^1\text{H})$  or  $\text{SiMe} \delta(^{13}\text{C})$  which resulted from the conversion of one silyl group to another were well behaved and did not depend on if the conversion was within a class or between classes (Table 4).<sup>61</sup> In general, replacing a Me group for a H shifted the  $\text{SiH} \delta(^1\text{H})$  and the  $\text{SiMe} \delta(^{13}\text{C})$  upfield, while replacing a Me group or a H with Cl shifted the  $\text{SiH} \delta(^1\text{H})$  and the  $\text{SiMe} \delta(^{13}\text{C})$  downfield, similar to the substituent trends observed for the  $\delta(^{29}\text{Si})$  of the silyl group.

The resonances of the  $\text{PMe}_3$  group in the  $^{31}\text{P}$  NMR spectra of complexes **1–10** did not exhibit a dependence on the number of chlorines present on silicon. A plot of  $\text{PMe}_3 \delta(^{31}\text{P})$  as a function of  $\Sigma\chi_i$  for the ruthenium silyl complexes can be found in Figure 6. The  $^{31}\text{P}$  NMR resonances were observed in the 8–13 ppm range and exhibit a nearly linear but inverse relationship with  $\Sigma\chi_i$ .

**3. NMR Coupling Constants.** Two sets of coupling constants were readily accessible from the NMR spectroscopic data:  $^2 J_{\text{SiP}}$  and  $^1 J_{\text{SiH}}$ . The  $^2 J_{\text{SiP}}$  values for the ruthenium silyl complexes were in the range 25–45 Hz, and a plot of  $^2 J_{\text{SiP}}$  as a function of  $\Sigma\chi_i$  can be found in Figure 7. This plot shows a nearly linear relationship with  $\Sigma\chi_i$ . The magnitude of the coupling constant  $^2 J_{\text{SiP}}$  increases as the electron-withdrawing ability of the substituents on silicon increases, consistent with Bent’s rule.<sup>60</sup> An increase in the s character in the Ru–Si bond (with increasing  $\Sigma\chi_i$ ) results in this bond becoming stronger, which in turn increases the communication (coupling) between silicon and phosphorus. Thus, the

(61) The ruthenium silyl complexes plotted in Figure 4 could also be classified using two other sets of criteria. One set could be based on the number of hydrogens on silicon to give a trihydrosilyl class, a dihydrosilyl class, and a monohydrosilyl class. The other set could be based on the number of methyl groups on silicon to give a dimethylsilyl class, a monomethylsilyl class, and a “non-methylsilyl” class. The ability to use different criteria to classify the silyl groups probably explains why  $^1\text{H}$  and  $^{13}\text{C}$  chemical shift changes are so well behaved compared to  $^{29}\text{Si}$  chemical shift changes upon H/Cl, H/Me, and Cl/Me exchanges (see text). All substituent exchanges can be viewed as conversions within a silyl class just by changing the classification criteria. A classification criterion based on the number of chlorines on silicon is used throughout this paper for internal consistency.

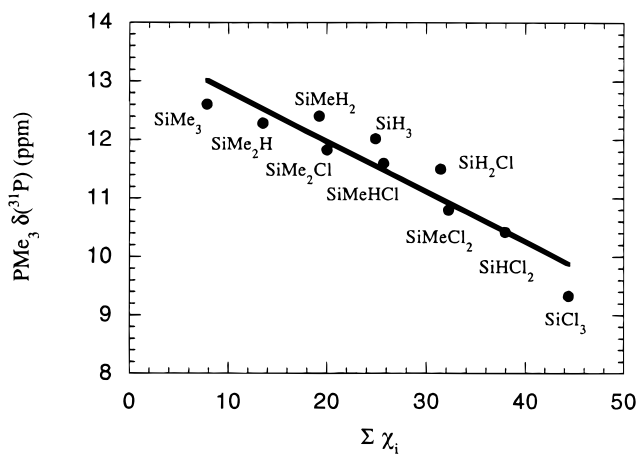


**Figure 6.**  $^{31}\text{P}$  NMR chemical shift of the  $\text{PMe}_3$  groups versus  $\Sigma\chi_i$  for the ruthenium silyl complexes  $\text{Cp}(\text{PMe}_3)_2\text{-RuSiR}_3$  (**1–10**): slope =  $-0.086$  ppm per  $\chi_i$  unit,  $R = 0.935$ .

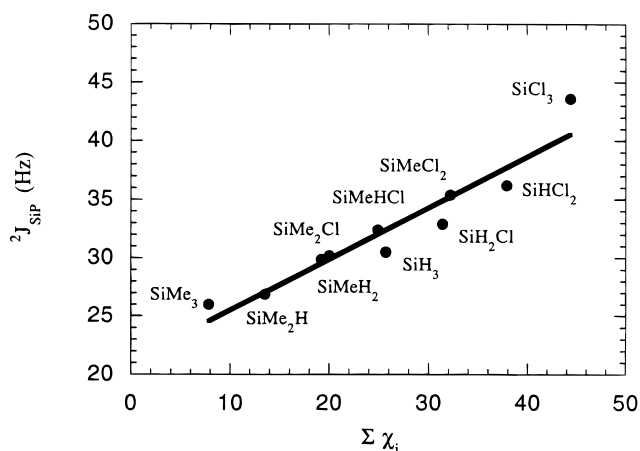


**Figure 7.**  $^2J_{\text{SiP}}$  (Hz) versus  $\Sigma\chi_i$  for the ruthenium silyl complexes  $\text{Cp}(\text{PMe}_3)_2\text{-RuSiR}_3$  (**1–10**): slope =  $0.44$  Hz per  $\chi_i$  unit,  $R = 0.953$ .

$\text{SiCl}_3$  complex has the largest  $^2J_{\text{SiP}}$  value, while the  $\text{SiMe}_3$  complex has the smallest  $^2J_{\text{SiP}}$  value.

Assuming Bent's rule holds for the other substituents on silicon, a similar trend should be observed for the other coupling constant  $^1J_{\text{SiH}}$ . The  $^1J_{\text{SiH}}$  values for the ruthenium hydrosilyl complexes were in the range 140–200 Hz, and a plot of  $^1J_{\text{SiH}}$  as a function of  $\Sigma\chi_i$  can be found in Figure 8. A rough linear relationship is observed between  $^1J_{\text{SiH}}$  and  $\Sigma\chi_i$ , consistent with Bent's rule. The effects on  $^1J_{\text{SiH}}$  of replacing one substituent with another are listed in Table 4. In all of the exchange cases, replacing an electropositive group (Me) or atom (H) with a more electronegative atom (H or Cl) results in an increase in  $^1J_{\text{SiH}}$ .

**D. Silyl Group Classifications.** From the plots in Figures 3–5, it is apparent that the grouping of ruthenium silyl complexes **1–10** into different classes (dichlorosilyl, monochlorosilyl, and “non-chlorosilyl”) is dependent on the number of chlorides on silicon. The chloride substituents influence the spectroscopic properties of these ruthenium silyl complexes beyond the electronic contributions which can be accounted for using Tolman's  $\chi_i$  parameter. This “chloride effect” has limited range and is most predominate in the NMR resonances of silicon and nuclei attached to silicon (H, C). Very little, if any, contribution from the “chloride

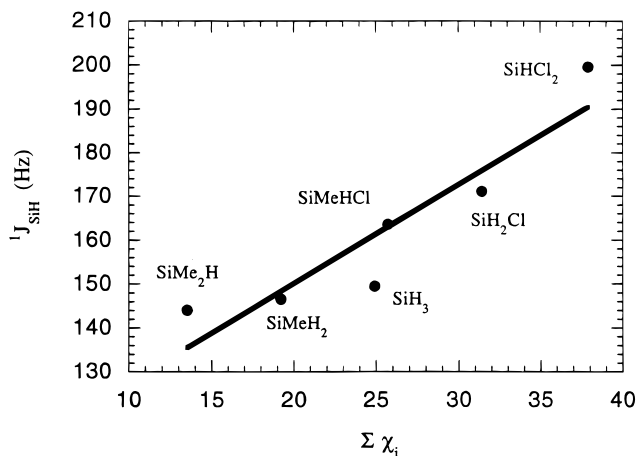
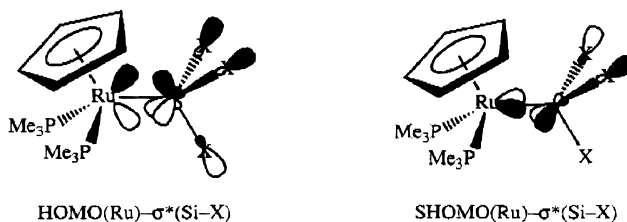


**Figure 8.**  $^1J_{\text{SiH}}$  (Hz) versus  $\Sigma\chi_i$  for the ruthenium hydrosilyl complexes  $\text{Cp}(\text{PMe}_3)_2\text{-RuSiHR}_2$ : slope =  $2.25$  Hz per  $\chi_i$  unit,  $R = 0.925$ .

**Scheme 1**



effect” is observed in the NMR resonances of phosphorus, two bonds from silicon, and the SiH and SiP coupling constants.

The differentiation of ruthenium silyl complexes **1–10** into the three silyl classes by the “chloride effect” can be rationalized by  $\pi$ -back-bonding from the  $d^6$  ruthenium center to the silyl group. In a main group element like silicon, the d orbitals are too diffuse and high in energy to play a significant role in  $\pi$ -back-bonding with a metal center.<sup>62–64</sup> On the other hand, the Si–X (X = H, Me, Cl)  $\sigma^*$  orbitals of the silyl group would have the appropriate symmetry for  $\pi$ -back-bonding with the ruthenium center. Linear combinations of the Si–X  $\sigma^*$  orbitals of  $\text{SiX}_3$  give an  $a_1$  and an e set, assuming  $C_{3v}$  localized symmetry. The doubly degenerate e set has the correct symmetry to interact with the HOMO and the SHOMO (second highest occupied molecular orbital) of the  $\text{Cp}(\text{PMe}_3)_2\text{Ru}$  moiety,<sup>65</sup> as shown in Scheme 1. The short Ru–Si and long Si–Cl distances observed in the solid-state structure of **1** (Figure 1) offer good supporting evidence for the  $d(\text{Ru})-\sigma^*(\text{Si}-\text{X})$   $\pi$ -back-bonding described in Scheme 1.

The presence of  $d(\text{Ru})-\sigma^*(\text{Si}-\text{X})$   $\pi$ -back-bonding explains the differentiation of the ruthenium silyl complexes into the three classes. Recently, ab initio calculations and natural bond order (NBO) analyses on a series of osmium silyl complexes,  $\text{Os}(\text{SiX}_3)\text{Cl}(\text{CO})\text{-}(\text{PPh}_3)_2$ , revealed an increasing importance in  $d(\text{Os})-\sigma^*(\text{Si}-\text{X})$   $\pi$ -bonding in the order  $\text{SiMe}_3 < \text{Si}(\text{OH})_3 <$

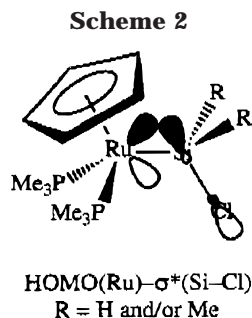
(62) Massey, A. G. *Main Group Chemistry*; Ellis Horwood: New York, 1990; Chapter 1.

(63) Kutzelnigg, W. *Angew. Chem., Int. Ed. Engl.* **1984**, *23*, 272–295.

(64) Orpen, A. G.; Connelly, N. G. *J. Chem. Soc., Chem. Commun.* **1985**, 1310–1311.

(65) Kostic, N. M.; Fenske, R. F. *Organometallics* **1982**, *1*, 974–982.





$\text{SiCl}_3 < \text{SiF}_3$ .<sup>55</sup> Thus, in the present study,  $d(\text{Ru})-\sigma^*(\text{Si}-\text{X})$   $\pi$ -back-bonding should be least prevalent with Me and H substituents on silicon and most prevalent with Cl substituents on silicon. Therefore, very little  $d(\text{Ru})-\sigma^*(\text{Si}-\text{X})$   $\pi$ -back-bonding is expected in the “non-chlorosilyl” class. The  $d(\text{Ru})-\sigma^*(\text{Si}-\text{X})$   $\pi$ -back-bonding in the monochlorosilyl class would be dominated by the  $d(\text{Ru})-\sigma^*(\text{Si}-\text{Cl})$  interaction (Scheme 2) which would be most favorable with the HOMO of the ruthenium moiety. In the dichlorosilyl class, the  $d(\text{Ru})-\sigma^*(\text{Si}-\text{X})$   $\pi$ -back-bonding would be dominated by the interaction of the ruthenium moiety HOMO and SHOMO with linear combinations of  $\sigma^*(\text{Si}-\text{Cl})$  (similar to those described in Scheme 1).

The presence of  $d(\text{Ru})-\sigma^*(\text{Si}-\text{Cl})$   $\pi$ -back-bonding would introduce some silylene character into the Ru-Si bond. In the <sup>29</sup>Si NMR spectrum, the resonances for the silicon center of base-free metal silylene complexes have been observed around 300 ppm.<sup>66,67</sup> Thus, even a small amount of silylene character due to  $d(\text{Ru})-\sigma^*(\text{Si}-\text{Cl})$   $\pi$ -back-bonding should dramatically shift downfield the observed  $\delta(^{29}\text{Si})$  for monochlorosilyl and dichlorosilyl groups compared to the  $\delta(^{29}\text{Si})$  of the “non-chlorosilyl” groups. This is nicely illustrated in Figure 3, where, in general,  $\delta(^{29}\text{Si})$  for the dichlorosilyl class is more downfield than the  $\delta(^{29}\text{Si})$  for the monochlorosilyl class, which is more downfield than the  $\delta(^{29}\text{Si})$  for the “non-chlorosilyl” class. The most dramatic evidence for the presence of  $d(\text{Ru})-\sigma^*(\text{Si}-\text{Cl})$   $\pi$ -back-bonding in the ruthenium silicon bond comes from examining the  $\delta(^{29}\text{Si})$  for complexes with nearly the same  $\sum\chi_i$  value. The “non-chlorosilyl”/monochlorosilyl pairs **7** ( $\text{SiH}_3$ ,  $\sum\chi_i = 24.9$ )/**5** ( $\text{SiMeHCl}$ ,  $\sum\chi_i = 25.7$ ) and **8** ( $\text{SiMeH}_2$ ,  $\sum\chi_i = 19.2$ )/**6** ( $\text{SiMe}_2\text{Cl}$ ,  $\sum\chi_i = 20.0$ ) are separated,  $\Delta\delta(^{29}\text{Si})$ , by 114 and 101 ppm, respectively, and suggest the presence of significant silylene character at silicon. The silylene character at silicon increases even more when a second chloride is added, as is evident in the monochlorosilyl/dichlorosilyl pair **3** ( $\text{SiH}_2\text{Cl}$ ,  $\sum\chi_i = 31.4$ )/**4** ( $\text{SiMeCl}_2$ ,  $\sum\chi_i = 32.2$ ) with  $\Delta\delta(^{29}\text{Si}) = 56$  ppm. It is interesting to note the smaller  $\Delta\delta(^{29}\text{Si})$  due to the second chloride on silicon and that a third chloride on silicon does not generate a new silyl class.

### Summary

The first series of transition metal silyl complexes,  $\text{Cp}(\text{PMe}_3)_2\text{RuSiR}_3$ , which contain all possible combinations of H, Cl, or Me groups on silicon has been

prepared. The nature of the substituents on silicon greatly effect the spectroscopic properties of these silyl complexes. NMR coupling constants,  $^2J_{\text{SiP}}$  and  $^1J_{\text{SiH}}$ , and Si-H stretching frequencies increase in magnitude as the electron-withdrawing ability of the substituents on silicon increases, consistent with Bent's rule. However, examination of <sup>29</sup>Si, <sup>1</sup>H(SiH), and <sup>13</sup>C(SiMe) chemical shifts indicates that the silyl groups are differentiated into three different classes: a dichlorosilyl class ( $\text{SiCl}_2\text{R}$ ), a monochlorosilyl class ( $\text{SiClR}_2$ ), and a “non-chlorosilyl” class ( $\text{SiR}_3$ ). This silyl group classification is due to  $\pi$ -back-bonding between the filled HOMO and SHOMO orbitals of the ruthenium moiety and the empty  $\sigma^*$  orbitals of the silicon-chlorine bonds.

### Experimental Section

**General Procedures.** All manipulations of oxygen- or water-sensitive compounds were carried out either under an atmosphere of argon by using Schlenk or vacuum-line techniques or under a helium/argon atmosphere in a Vacuum Atmospheres glovebox.<sup>68</sup> <sup>1</sup>H NMR (250 MHz), <sup>13</sup>C{<sup>1</sup>H} NMR (62.9 MHz), and <sup>31</sup>P{<sup>1</sup>H} NMR (101.3 MHz) spectra were recorded on a Bruker AC-250 spectrometer. <sup>29</sup>Si DEPT NMR (79.5 MHz) spectra were recorded on a Varian VXR 400S spectrometer. The  $\text{PMe}_3$  resonances in these compounds did not appear as a simple first-order pattern in the <sup>1</sup>H NMR, but as a  $A_9XX'A'_9$  pattern, the appearance of which was a “filled-in-doublet” (fd) with the separation of the outer lines  $N = ^2J_{\text{PH}} + ^4J_{\text{PH}}$ .<sup>69,70</sup> Likewise, in the <sup>13</sup>C{<sup>1</sup>H} NMR, the  $\text{PMe}_3$  resonances appeared as a virtual triplet (vt) with the separation of the outer lines  $N = ^1J_{\text{PC}} + ^3J_{\text{PC}}$ .<sup>69,70</sup> The <sup>1</sup>H chemical shifts were referenced to the residual proton peak of the solvent  $\text{CDHCl}_2$  (5.32 ppm). The <sup>13</sup>C chemical shifts were referenced to the central peak of  $\text{CD}_2\text{Cl}_2$  (53.8 ppm). The <sup>29</sup>Si chemical shifts were referenced to external  $\text{SiMe}_4$  (0.00 ppm). The <sup>31</sup>P chemical shifts were referenced to external  $\text{H}_3\text{PO}_4$  (85%, 0.00 ppm). IR spectra were recorded on a Perkin-Elmer 1600 Series FT-IR spectrometer. The multinuclear NMR and IR data are summarized in Table 1. Electron-impact mass spectra were obtained with a Hewlett-Packard 5988A GC-MS instrument. Elemental analyses were carried out by Oneida Research Services (Whitesboro, NY). Mass spectrum and elemental analysis data are summarized in Table 2.

**Materials.**  $\text{Cp}(\text{PMe}_3)_2\text{RuH}^{38}$  was prepared by the literature method.  $\text{AlMe}_3$  (2 M in toluene, Aldrich) was used as received. Chlorosilanes were stored over  $\text{CaH}_2$  and vacuum transferred immediately prior to use. Anhydrous diethyl ether and hexanes were stored over  $[\text{Cp}_2\text{TiCl}]_2\text{ZnCl}_2^{71}$  and vacuum transferred immediately prior to use. Dichloromethane was distilled from and stored over  $\text{CaH}_2$  and vacuum transferred immediately prior to use. Dichloromethane-*d*<sub>2</sub> was dried over  $\text{P}_2\text{O}_5$  and stored over  $\text{CaH}_2$ .

**$\text{Cp}(\text{PMe}_3)_2\text{RuSiR}_2\text{Cl}$  [ $\text{SiR}_2\text{Cl} = \text{SiCl}_3$  (**1**),  $\text{SiHCl}_2$  (**2**),  $\text{SiH}_2\text{Cl}$  (**3**)].** These ruthenium silyl complexes were prepared by the reaction of  $\text{Cp}(\text{PMe}_3)_2\text{RuH}$  with chlorosilanes in  $\text{Et}_2\text{O}$ . In a typical reaction, excess  $\text{H}_2\text{SiCl}_2$  (0.53 mmol) was added by vacuum transfer to a cold ( $-78^\circ\text{C}$ ) solution of  $\text{Cp}(\text{PMe}_3)_2\text{RuH}$  (225 mg, 0.70 mmol) in  $\text{Et}_2\text{O}$ . The precipitate that formed was isolated by filtration, washed with hexanes, and dried under vacuum to afford  $[\text{Cp}(\text{PMe}_3)_2\text{RuH}_2]\text{Cl}$  as a white solid in 104% yield (130 mg). The filtrate was evaporated to dryness

(68) Shriver, D. F.; Drezdson, M. A. *The Manipulation of Air-Sensitive Compounds*, 2nd ed.; Wiley-Interscience: New York, 1986.

(69) Harris, R. K. *Can. J. Chem.* **1964**, *42*, 2275–2281.

(70) Harris, R. K.; Hayter, R. G. *Can. J. Chem.* **1964**, *42*, 2282–2291.

(71) Sekutowski, D. G.; Stucky, G. D. *Inorg. Chem.* **1975**, *14*, 2192–2199.

(66) Straus, D. A.; Grumbine, S. D.; Tilley, T. D. *J. Am. Chem. Soc.* **1990**, *112*, 7801–7802.

(67) Grumbine, S. K.; Tilley, T. D.; Arnold, F. P.; Rheingold, A. L. *J. Am. Chem. Soc.* **1994**, *116*, 5495–5496.

to give **3** as a yellow solid in 81% yield (110 mg). Isolated yields for ruthenium silyl complexes **1–3** were in the 80–90% range.

**Cp(PMe<sub>3</sub>)<sub>2</sub>RuSiRMeCl [SiRMeCl = SiMeCl<sub>2</sub> (**4**), SiMeHCl (**5**), SiMe<sub>2</sub>Cl (**6**)]**. These ruthenium silyl complexes were prepared by the reaction of Cp(PMe<sub>3</sub>)<sub>2</sub>RuH with chloromethylsilanes in CH<sub>2</sub>Cl<sub>2</sub>, since the reactions of Cp(PMe<sub>3</sub>)<sub>2</sub>RuH with these chloromethylsilanes in Et<sub>2</sub>O were slow and incomplete. Excess chloromethylsilane (~1 equiv) was added by vacuum transfer to a solution of Cp(PMe<sub>3</sub>)<sub>2</sub>RuH in CH<sub>2</sub>Cl<sub>2</sub> cooled to -78 °C. The reaction mixture was allowed to warm to room temperature and stirred for 1 h. The reaction volatiles were removed under vacuum. The reaction residue was extracted with hexane and the hexane solution filtered through a glass frit. Extraction was continued until the hexane extracts were colorless. The white solid that remained was vacuum-dried to give [Cp(PMe<sub>3</sub>)<sub>2</sub>RuH<sub>2</sub>]Cl in >90% yields. The hexane extracts were combined and evaporated to dryness to give the corresponding silyl complexes **4–6** as yellow air- and water-sensitive solids in 60–85% yields.

**Cp(PMe<sub>3</sub>)<sub>2</sub>RuSiR<sub>2</sub>H and Chlorosilanes with NEt<sub>3</sub>**. Ruthenium silyl complexes **1**, **5**, and **6** were prepared by the reaction of Cp(PMe<sub>3</sub>)<sub>2</sub>RuH with chlorosilanes in CH<sub>2</sub>Cl<sub>2</sub> in the presence of excess NEt<sub>3</sub>. In a typical reaction, excess MeSiHCl<sub>2</sub> (1.4 equiv) was added by vacuum transfer to a solution of Cp(PMe<sub>3</sub>)<sub>2</sub>RuH (340 mg, 1.07 mmol) and NEt<sub>3</sub> (0.75 mL, ~5 equiv) in CH<sub>2</sub>Cl<sub>2</sub> (25 mL). The reaction mixture was stirred at room temperature for 1–2 h. The reaction volatiles were removed under vacuum. The reaction residue was extracted with Et<sub>2</sub>O/hexane (1:1), and the extract solution was filtered through a Celite plug to remove the insoluble [HNEt<sub>3</sub>]Cl. The filtrate solution was evaporated to dryness to give silyl complex **5** as light yellow air- and water-sensitive solid (402 mg, 95%). Similar yields were obtained for silyl complexes **1** and **6**.

**Cp(PMe<sub>3</sub>)<sub>2</sub>RuSiR<sub>2</sub>H [SiR<sub>2</sub>H = SiH<sub>3</sub> (**7**), SiMeH<sub>2</sub> (**8**), SiMe<sub>2</sub>H (**9**)]**. These hydrosilyl ruthenium complexes were prepared from the reaction of LiAlH<sub>4</sub> with the corresponding chlorosilyl ruthenium complexes. In a typical reaction, Et<sub>2</sub>O (15 mL) was added by vacuum transfer to a flask charged with **6** (585 mg, 1.42 mmol) and LiAlH<sub>4</sub> (60 mg, 1.58 mmol). The reaction mixture was stirred overnight at room temperature under an Ar atmosphere. Removal of the volatiles under vacuum gave a gray residue, which was extracted with hexanes (2 × 15 mL). The hexane extracts were filtered through Celite and evaporated to dryness to give **9** as a yellow solid (478 mg, 89%). Complex **8** was prepared in a similar manner from the reaction of either **4** or **5** with LiAlH<sub>4</sub> in Et<sub>2</sub>O. The reaction of **1**, **2**, or **3** with LiAlH<sub>4</sub> in Et<sub>2</sub>O was used to prepare **7**. Typical yields of hydrosilylruthenium complexes **7–9** were in the 80–90% range.

**Cp(PMe<sub>3</sub>)<sub>2</sub>RuSiMe<sub>3</sub> (**10**)**. AlMe<sub>3</sub> (0.6 mL, 1.2 mmol) was added by syringe to a cold (-78 °C) slurry of **6** (505 mg, 1.2 mmol) in toluene (25 mL) under argon. Upon addition of the AlMe<sub>3</sub>, complex **6** dissolved to give a light green solution, which turned yellow as the solution warmed to room temperature. After 30 min, the volatiles were removed under vacuum to give a yellow residue, which was extracted with hexanes (2 × 10 mL). The hexane extracts were filtered through Celite and evaporated to dryness. The residue was sublimed at 100 °C (<0.03 mmHg) to afford **10** as a tan solid in 86% yield (414 mg). Resublimation (80 °C, <0.03 mmHg) of the tan solid gave **10** as an analytically pure, yellow-orange solid (378 mg, 79%).

**Structure Determination of Cp(PMe<sub>3</sub>)<sub>2</sub>RuSiCl<sub>3</sub> (**1**)**. Crystals of **1** suitable for X-ray diffraction analysis were grown in a sealed glass tube by slowly cooling a saturated toluene/hexanes solution of **1** from 80 °C to room temperature. Intensity data were collected on a Syntex P2<sub>1</sub> diffractometer using Mo Kα (λ = 0.710 73 Å) radiation. The structure was solved using a combination of direct methods and difference

**Table 5. Crystal Data, Data Collection, and Refinement Parameters for Cp(PMe<sub>3</sub>)<sub>2</sub>RuSiCl<sub>3</sub> (**1**)**

empirical formula	C <sub>11</sub> H <sub>23</sub> Cl <sub>3</sub> P <sub>2</sub> RuSi
fw	452.74
cryst syst	monoclinic
space group	P2 <sub>1</sub>
<i>a</i> (Å)	8.455(3)
<i>b</i> (Å)	8.820(3)
<i>c</i> (Å)	12.436(4)
β (deg)	90.35(3)
<i>V</i> (Å <sup>3</sup> )	927.4(6)
<i>Z</i>	2
<i>d</i> <sub>calcd</sub> (Mg m <sup>-3</sup> )	1.621
radiation, λ (Å)	graphite monochromator Mo Kα, 0.710 73
μ, abs coeff (mm <sup>-1</sup> )	1.498
cryst dimens (mm)	0.20 × 0.20 × 0.20
temp (K)	141(2)
<i>F</i> (000)	456
2θ range for data collection (deg)	4.82–55.00
index ranges	-1 ≤ <i>h</i> ≤ 10, -11 ≤ <i>k</i> ≤ 11, -16 ≤ <i>l</i> ≤ 16
no. of refls collected	5104
no. of ind refls	4255 ( <i>R</i> <sub>int</sub> = 0.0332)
refinement method	full-matrix least-squares on <i>F</i> <sup>2</sup>
no. of data/restraints/params	4255/1/163
goodness-of-fit on <i>F</i> <sup>2</sup> <sup>a</sup>	1.193
final <i>R</i> indices [ <i>I</i> > 2σ( <i>I</i> )] <sup>b,c</sup>	<i>R</i> 1 = 0.0476, w <i>R</i> 2 = 0.1094
<i>R</i> indices (all data) <sup>b,c</sup>	<i>R</i> 1 = 0.0536, w <i>R</i> 2 = 0.1119
absolute struct param	0.01(6)
largest diff peak and hole (e Å <sup>-3</sup> )	0.929 and -1.292

<sup>a</sup> *S* = [Σ[w(*F*<sub>o</sub><sup>2</sup> - *F*<sub>c</sub><sup>2</sup>)]/(*n* - *p*)<sup>1/2</sup>. The goodness of fit is based on *F*<sup>2</sup> where *n* = number of data and *p* = number of parameters refined. <sup>b</sup> *R*1 = Σ||*F*<sub>o</sub>|| - ||*F*<sub>c</sub>||/Σ||*F*<sub>o</sub>||. Conventional *R* factors are calculated using the observed criterion. This criterion is irrelevant to the choice of reflections used in the refinement. <sup>c</sup> w*R*2 = [Σ[w(*F*<sub>o</sub><sup>2</sup> - *F*<sub>c</sub><sup>2</sup>)]/Σ[w(*F*<sub>o</sub><sup>2</sup>)]<sup>1/2</sup>. Weighted *R*-factors are based on *F*<sup>2</sup> and are statistically about twice as large as those based on *F*.

Fourier syntheses (SHELXTL Plus)<sup>72</sup> and was refined on |*F*<sub>o</sub><sup>2</sup>| using full-matrix least-squares. All hydrogen atoms were placed in calculated positions and refined using a riding model. All non-hydrogen atoms were refined anisotropically. Refinement of 163 parameters against all 4255 unique data (*R*<sub>int</sub> = 3.32%) with one restraint yielded an *R* index, w*R*2, of 11.19% (*R*1 = 4.76% for *I* > 2σ(*I*)) with a goodness of fit of 1.193. Crystallographic data and refinement parameters are listed in Table 5.

**Recovery of the Cp(PMe<sub>3</sub>)<sub>2</sub>Ru Moiety**. The Cp(PMe<sub>3</sub>)<sub>2</sub>-Ru moiety can be recovered from ruthenium silyl complexes **1–10** or other waste materials (failed reactions, decomposed samples, NMR samples, etc.) by the following method. MeOH was added by vacuum transfer to a flask charged with Cp(PMe<sub>3</sub>)<sub>2</sub>Ru containing material and equipped with a reflux condenser. A large excess of Na metal was added to the MeOH solution. The mixture was heated to reflux for 3 h, and the reaction volatiles were removed under vacuum. The residue was extracted with hexanes until the extracts were colorless. The hexane extracts were filtered through Celite and evaporated to dryness. Sublimation (80 °C, <0.03 mmHg) of the resulting mixture afforded a yellow-orange waxy solid, which was a mixture of Cp(PMe<sub>3</sub>)<sub>2</sub>RuH, Cp(PMe<sub>3</sub>)<sub>2</sub>RuSi(OMe)<sub>3</sub>, and/or Cp(PMe<sub>3</sub>)<sub>2</sub>RuSiRR'R'' (*R*, *R'*, *R''* = H, Me, and/or OMe); the distribution of ruthenium-containing species depended on the initial composition of the original Cp(PMe<sub>3</sub>)<sub>2</sub>Ru waste material. The sublimate was dissolved in Et<sub>2</sub>O, and triflic acid (TfOH) was added dropwise until no more white precipitate formed upon addition of TfOH. The precipitate was isolated by filtration, washed with Et<sub>2</sub>O, and dried under vacuum to give the ruthenium dihydride [Cp(PMe<sub>3</sub>)<sub>2</sub>RuH<sub>2</sub>]OTf<sup>38</sup> as a white solid. [Cp(PMe<sub>3</sub>)<sub>2</sub>RuH<sub>2</sub>]OTf was then reacted with NaOMe (8 equiv) in refluxing MeOH for 2 h. The volatiles were removed

(72) SHELXTL PLUS Software Package for the Determination of Crystal Structures, Version 5.0; Siemens Analytical X-ray Instruments, Inc.: Madison, WI, 1994.

under vacuum, and the residue was extracted with hexanes until the extracts were colorless. The hexane extracts were filtered through Celite and evaporated to dryness. Sublimation of the residue (60 °C, <0.03 mmHg) afforded Cp(PMe<sub>3</sub>)<sub>2</sub>RuH<sup>38</sup> as a yellow, air-sensitive solid in >80% yield (based on [Cp-(PMe<sub>3</sub>)<sub>2</sub>RuH<sub>2</sub>]OTf).

**Acknowledgment** is made to the Baker Fund and Research Challenge Program at Ohio University for financial support of this research, and Johnson Matthey for the generous loan of RuCl<sub>3</sub>·*n*H<sub>2</sub>O. F.R.L. would also like to thank Drs. Cathy Sultany, Kevin M. Kane, and

Leo Liu for help in obtaining <sup>29</sup>Si NMR spectra, and Brandon T. Weldon for help in preparing some of the ruthenium silyl complexes. Also, we would like to thank a referee for helpful suggestions.

**Supporting Information Available:** Tables of crystal data, collection, and refinement parameters, positional and anisotropic displacement parameters, and interatomic distances and angles for Cp(PMe<sub>3</sub>)<sub>2</sub>RuSiCl<sub>3</sub> (**1**). This material is available free of charge via the Internet at <http://pubs.acs.org>.

OM980951+